ELSEVIER

Thermal and mechanical properties of ceramic blanket particle bed materials: Numerical derivation

Mohamed Abdou [*], Alice Ying, Zi Lu

43-133 Engineering IV, Institute of Plasma and Fusion Research, Mechanical and Aerospace Engineering Department, 44-114, Engineering IV, University of California, Los Angeles CA 90095-1597, USA

Abstract

In this paper, recent work on the modeling for predicting the effective thermal and mechanical properties of the ceramic breeder blanket particle bed materials is presented. The model is based on the micromechanics displacement method in conjunction with an iterative process of the successive releasing of fixing vectors. It serves as an useful tool to study the blanket thermomechanical state under prototypical conditions. The stress and strain relationship of the sphere-pac bed under an applied external constraint was studied. In addition, the model was applied to the analysis of stress exerted on the container wall due to bed thermal expansion, while calculations were made to estimate the bed effective modulus and mean thermal expansion coefficient. Further development of this computer simulation model is recommended. © 1998 Elsevier Science B.V. All rights reserved.

1. Introduction

In an effort to evaluate the maximum stress levels to which bed particles and clad wall are subjected, the stress-strain behavior of the solid breeder blanket particle bed materials have been experimentally studied [1,2]. A series of uniaxial compression tests were performed in an INSTRON hydraulic-press test facility in which compressive loads are applied to Li_2ZrO_3 packed beds. The experimental data shows that mechanical properties such as the bed effective modulus are stress dependent. Specifically, the bed effective modulus is about two orders of magnitude lower than that of the solid material. On the other hand, analysis concerning blanket particle bed thermomechanical interaction during reactor operation based on the continuum approach has shown that the stress caused by the high thermal expansion of the breeder particle bed material could lead to ceramic particle breakage if the bed behaves like the solid material. The calculation also shows that the clad deformation caused by this stress could lead to a possible bed/clad separation which would add an unfavorable thermal resistance to the region and increase local temperature. These results provided preliminary information regarding the order of the magnitude in terms of effective bed modulus and the overall stress state. Yet they are not prototypical while better quantification is needed.

It is desirable to describe the thermomechanical behavior of packed bed materials using continuum variables such as strain and stress. However, this transformation from a complicated discrete system to a simpler continuum system results in certain information being lost. To remedy this deficiency and better quantify bed effective thermal and mechanical properties, a numerical model for simulating packed bed thermomechanical behavior is currently underdevelopment and is described in Section 2. The use of this model to estimate the wall loading of the clad due to bed thermal expansion is also described. In addition, the effective bed thermal expansion coefficient and elastic modulus are derived based on the macroscopic thermomechanical state of the assembly and are presented in Section 3.

2. Numerical simulation of packed bed ceramic breeder materials

The thermomechanical behavior of a packed bed material can be analyzed using two approaches that

* Corresponding author. Tel.: +1-310-2060501; fax: +1-310-8252599; e-mail: abdou@fusion.ucla.edu.

account for the particulate structure and the particle interaction, namely, the discrete computer simulation approach and the homogenization approach. Both approaches are used in conjunction with a micro-mechanics modelling scheme in which the particle bed is modeled as a collection of rigid particles interacting via Hertz–Mindlin type contact interactions of non-conforming bodies [3]. Because the discrete computer simulation approach can provide a wide range of valuable information not available by real experiments, it is preferred. Our initial effort is to develop a 2-dimensional model which can be expanded later for a 3-dimensional assembly.

2.1. The numerical model

The fundamental idea of the model is based on the algorithm developed by Kishino [4]. To attain the equilibrium state of the particle assembly, the model calculates the displacements of each particle independently of the others, meanwhile the particles are displaced according to stiffness of the contacts with neighboring particles. During each iterative step all particles are assumed to be fixed except one. The resultant external and contact forces acting on the particle are calculated and the displacement is determined. Then the next particle is considered (Fig. 1).

The basic unknowns are the displacements of the particles caused by the given external and internal loads. The model adopts Coulomb's friction law in order to limit the magnitude of the tangential component of the contact force [4], while the elastic behavior of a particle is described by the action of springs virtually attached at the contact point in the normal and tangential directions. The contact interaction provides a local constitutive relationship between the forces (n, $t =$ the normal and tangential force at the contact, respectively) at the contact and relative incremental movement of the contacting particles ($\Delta\delta_n$, $\Delta\delta_t$) via the stiffness as follows:
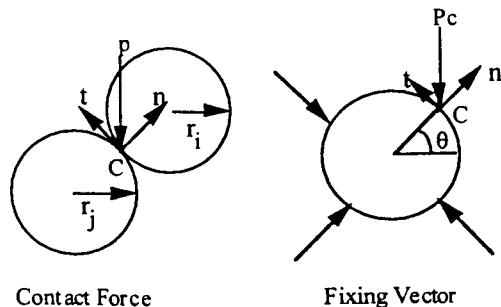
$$n = k_n \Delta\delta_n, \tag{1}$$

$$t = k_s \Delta\delta_s. \tag{2}$$

The contact stiffness, k_n and k_s, obtained from the Hertz–mindlin theory for frictional contacts are given as

$$\frac{1}{k_n} = \frac{(1 - v)}{2GA}, \tag{3}$$

$$\frac{1}{k_s} = \frac{(2 - v)}{4GA} \left[1 - \frac{n}{t \tan[\varphi_\mu]} \right]^{1/3}, \tag{4}$$

where

$$A = \left[\frac{3(1 - v)rn}{8G} \right]^{1/3} \tag{5}$$

and $G =$ shear modulus of the particle material; $v =$ Poisson's ratio; $r =$ particle radius; and $\varphi_\mu =$ friction angle between particles.

The equilibrium state of a particle assembly under a prescribed boundary condition is obtained by releasing the fixing vectors which consist of the forces required for fixing particles at their centers. For a single particle, it is calculated in terms of the contact force P_c applied at the contact point c and the body force B as

$$F = \sum_c T_c P_c - B. \tag{6}$$

where $\sum_c$ represents the summation over the contact points of a particle and T_c

$$T_c = \begin{bmatrix} \cos\theta & -\sin\theta \\ \sin\theta & \cos\theta \\ 0 & 1 \end{bmatrix}_c \tag{7}$$

is the transformation matrix.

Because an incremental movement of a particle will produce an incremental contact force as

$$\Delta P_c = S_c T_c^t \Delta x, \tag{8}$$

where

$$S_c = \begin{bmatrix} k_n & 0 \\ 0 & k_s \end{bmatrix}_c \tag{9}$$

and thus, the increment of fixing vector is expressed as follows:

$$\Delta F = S \Delta x, \tag{10}$$

where

$$S = \sum_c T_c S_c T_c^t \tag{11}$$

is the contact stiffness matrix which is defined as a set of additional fixing vectors required to give unit movements of a particle while other particles are fixed. The equilibrium condition for one particle is solved by releasing its fixing vector as follows:

$$F + \Delta F = 0, \tag{12}$$

which leads to $\Delta x = -S^{-1}F$ for the case det $S \neq 0$.

Fig. 1. Illustration of contact force and fixing vector used in the model development.

The assembly is assumed to be bounded by four rigid walls that form a rectangle in the initial state. The interaction between a boundary element and a particle is represented by virtual springs in a similar way as the interaction between two particles. The fixing vector of a boundary element consists of the external force and the external moment, whereas the contact stiffness of a boundary element is defined as the force required for unit movement of the boundary element with the neighboring particles being fixed. If a load increment is given, the algorithm searches for the equilibrium state of the assembly that corresponds to the contact stiffness matrix defined from the locations of neighboring particles. In the process of iteration, the contact stiffness matrix keeps changing with the relative movements of the particles. Nevertheless, it is kept constant during each iteration step. The iterative calculation is repeated until an equilibrium and compatible state of the assembly is found.

2.2. Results

2.2.1. Stress–strain relationship

Initially, the program searches for an equilibrium state of a particle assembly by utilizing a random number generator for a given size of a rectangular area, a total number of 110 particles, a constant average particle diameter, and a density function that defines the range of particle diameters. As a result, an assembly consisting of touching particles with zero contact forces is given and shown in Fig. 2.

Preliminary cases are performed for particles where the contacts have resistance to shear (i.e., $t =$ the frictional tangential force $= 0$) such as encountered in a perfectly smooth surface. The calculated result of the
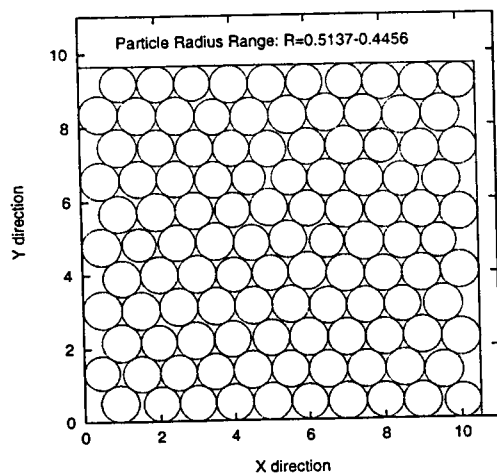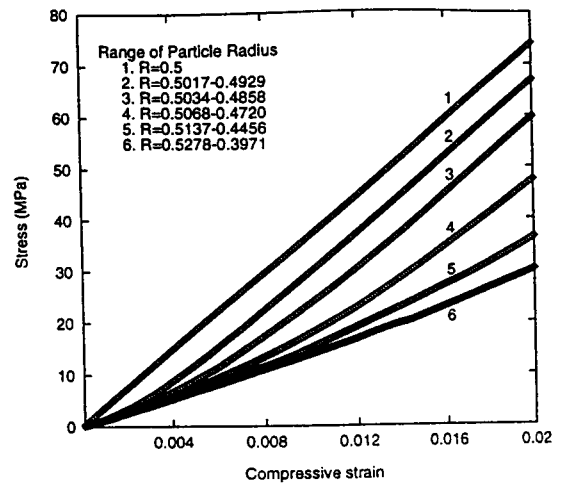

Fig. 3. Stress and strain relationship for various packing assemblies (aluminum particle bed arrangement, Young's modulus = 70 GPa; Poisson's ratio = 0.28).

average wall stress as a function of compressive strain is illustrated in Fig. 3 for different packing assemblies. It is interesting to note that an increase in the range of particle sizes leads to a decrease in wall stress and a lower effective modulus. This can be explained by examining the particle packing geometrical arrangement. As shown in Fig. 4, for a highly packed arrangement the center of the particle does not shift relative to the tangential coordinate under uniaxial normal compression. Conversely, the particle moves both in the x- and y directions if the bed is not fully packed initially due to a relatively large difference between R_{min} and R_{max} as shown in Fig. 5. These results point out that the presence of small particles facilitates the movement of bigger

Fig. 2. Initial packed state for a range of particle radii between 0.5137134 and 0.4455995 mm.
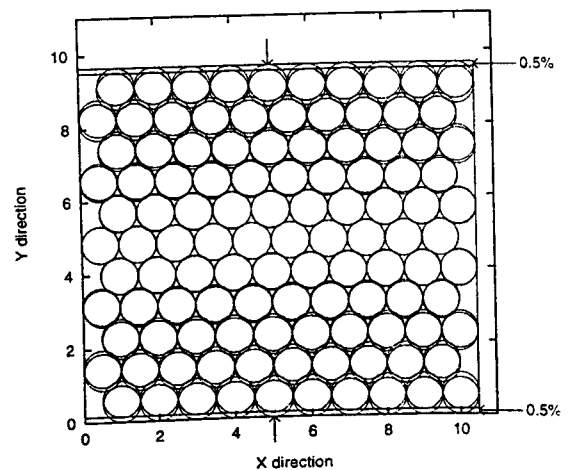

Fig. 4. Initial and final packed states under a total uniaxial compressive strain of 1% for a packed assembly using uniform particle size of 0.5 mm.
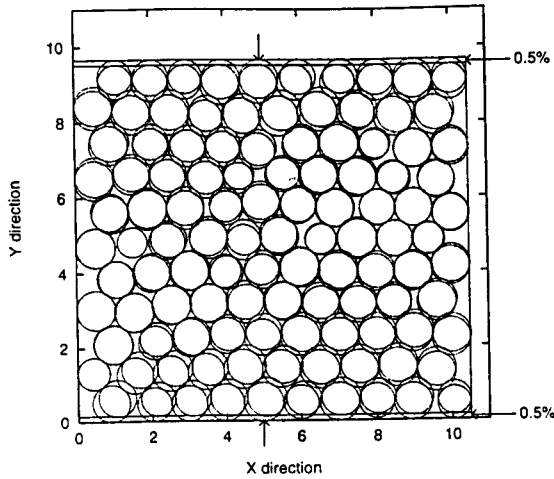
Fig. 5. Initial and final packed states under a total uniaxial compressive strain of 1% for a packed assembly using a range of particle sizes between 0.527803 and 0.3971179 mm.

particles, so large rearrangements are possible without significant forces being exerted. The effective modulus calculated according to the relationship between the incremental stress and the incremental strain approaches a constant value of about 3.5 GPa. This is reasonably close to previous experimental data of 2.2 GPa [2].

2.2.2. Stress distribution due to bed thermal expansion

The model as developed was applied to a blanket ceramic breeder particle bed to evaluate the maximum stress levels to which bed particles and wall are subjected due to bed thermal expansion (see Fig. 6 for the initial assembly). The relative displacement $\Delta\delta_n$ at the contact point as given in Eq. (1) due to thermal expansion is now calculated as

$$\Delta\delta_n = D_n - R_i(1 + \alpha\,\Delta T) - R_j(1 + \alpha\,\Delta T), \qquad (13)$$

where D_n = the initial distance between particle i and particle j along the normal direction, α = thermal expansion coefficient of particle material, R = particle radius and ΔT = bed temperature rise. The resultant stress, calculated as the force divided by area, exerted on the

wall along the x-plane due to bed thermal expansion for different rises in bed temperature is shown in Fig. 7. The stress magnitude as calculated is much higher than the stress level inducing the break-up of the ceramic particles as observed in previous experiments [1]. Clearly the model needs further development of incorporating the frictional tangential force and fracture criteria before definite conclusions can be drawn. Yet, it is noted that the stress near the wall deviates from that of the bulk value in response to local particle rearrangement. The stresses exerted on the wall for various bed temperature differences are shown in Fig. 8. As the temperature difference increases, the stress exerted on the hottest side of the wall drops slightly even it is kept at the same temperature. This is probably due to the fact that under such circumstances, the particles have more room to expand toward the cold side of the wall and thus reduce the stress level.

3. Derivation of effective bed thermal expansion coefficient

The mean effective bed thermal expansion coefficient is to be calculated as:

$$\alpha_p = \frac{\sigma(1 - v_p)}{E_p\Delta T}. \qquad (14)$$

where E_p, v_p are the particle bed effective modulus and Poisson's ratio (a value of 0.25 is used for the assumed hydrostatic frictionless particle bed), respectively. The bed effective modulus of 3.63 GPa for a highly packed state (packing as in Fig. 4) and of 2.0 GPa for a loose packed state (packing as in Fig. 5) as derived from the stress–strain relationships are used in the derivation. The mean effective bed thermal expansion coefficient based on Eq. (14) and the calculated macroscopic stress level due to bed thermal expansion shows no difference from that of the solid material. The possible factors contributing to this finding at this stage of the investigation might be due to the negligence of the frictional tangential forces at the contact points in addition to the 2-dimensional effect. Both affect the rearrangement of the particles and the distribution of contact forces.
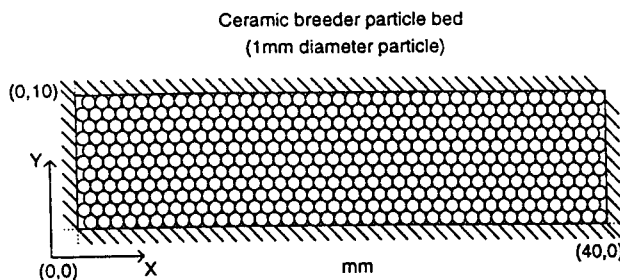

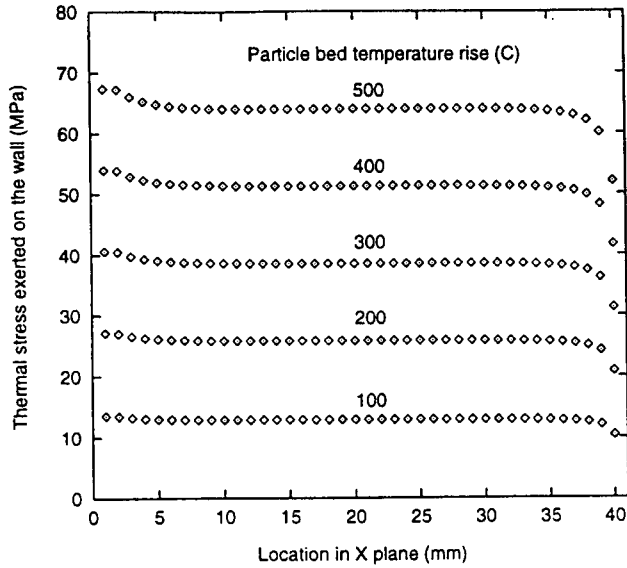Fig. 6. Initial packed state and boundary conditions for thermal stress calculations.

Fig. 7. Thermal stress exerted on the wall along the x-plane for different rises in bed temperature (Li₂ZrO₃ sphere-pac packed bed of 1 mm particle diameter; Young's modulus = 169 GPa for 12% porosity; Poisson's ratio = 0.2).
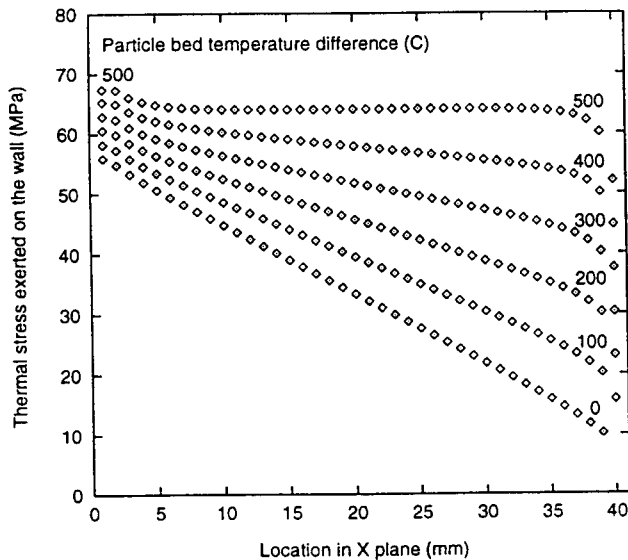

Fig. 8. Thermal stress exerted on the wall along the x-plane for different temperature differences across the bed (Li₂ZrO₃ sphere-pac packed bed of 1 mm particle diameter; Young's modulus = 169 GPa for 12% porosity; Poisson's ratio = 0.2).

4. Summary

A 2-D numerical model has been developed for the estimation of the thermomechanical state and effective thermal and mechanical properties of particle bed ceramic breeder blanket materials. The model is able to follow the rearrangement of the particles under external and internal loads. Loading processes are given as a series of load steps while an iteration method is used to find the equilibrated, compatible and physically correct state of the assembly for each load step. Preliminary calculations confirmed that the effective modulus of a sphere-pac bed material has a much lower magnitude than that of the solid material in addition to being packing and stress dependent. Yet the calculations showed that the effective bed thermal expansion coefficient is less packing sensitive for the smooth frictionless sphere particle beds.

References

[1] A. Ying, M.A. Abdou, Analysis of Thermomechanical Interactions and Properties of Ceramic Breeder Blankets, presented at ISFNT-4, Tokyo, Japan, to be published in Fusion Eng. Design.

[2] A. Ying, L. Zi, M.A. Abdou, Mechanical Behavior and Properties of Solid Breeder Blanket Packed Beds, presented at ISFNT-4, Tokyo, Japan, to be published in Fusion Eng. Design.

[3] R.D. Mindlin, H. Deresiewicz, Elastic Spheres in Contact Under Varying Oblique Forces, J. Appl. Mech. ASME 22 (3) (1953) 327–344.

[4] Y. Kishino, Disc model analysis of grannular media, in: M. Satake, J.T. Jenkins (Eds.), Micromechanics of Grannular Materials, Elsevier, Amsterdam, 1988, pp. 143–152.